Ultrafine particle and fine trace metal (As, Cd, Cu, Pb and Zn) pollution episodes induced by industrial emissions in Huelva, SW Spain

R. Fernández-Camacho [a,*], S. Rodríguez [a,b], J. de la Rosa [a], A.M. Sánchez de la Campa [a], A. Alastuey [c], X. Querol [c], Y. González-Castanedo [a], I. Garcia-Orellana [d], S. Nava [e]

[a] Joint Research Unit to CSIC "Atmospheric Pollution", CIQSO, University of Huelva, Campus El Carmen, E21071 Huelva, Spain
[b] Izaña Atmospheric Research Centre, AEMET Joint Research Unit to CSIC "Studies on Atmospheric Pollution", La Marina 20, planta 6, Santa Cruz de Tenerife, E38071 Canary Islands, Spain
[c] Institute of Environmental Assessment and Water Research IDAEA, CSIC, C/Jordi Girona, 18-26, 08034 Barcelona, Spain
[d] National Accelerator Center, Avd. Thomas A. Edison 7, E-41092 Sevilla, Spain
[e] Dipartimento di Fisica and INFN Sezione di Firenze, via Sansone 1, I- 50019 Sesto Fiorentino, Italy

HIGHLIGHTS

► We studied how industrial emissions contribute to ultrafine particles (UP).
► Traffic and industrial UP episodes are identified from the relation of UP and PM$_{2.5}$.
► Road traffic emissions, in the morning rush hours, are associated with OM and BC.
► Industrial plumes, during daylight, are related with heavy metals.
► Industrial emissions are the first cause of high UP in Huelva city.

ARTICLE INFO

ABSTRACT

Urban air quality impairment by ultrafine particles has become a matter of concern due to the adverse effects on human health. Most of the studies of ultrafine particles in urban air quality have focused on vehicle exhaust emissions. We studied how industrial emissions contribute to ultrafine particle concentrations in downwind urban ambient air. This research is based on experimental data collected in the ambient air of the industrial city of Huelva (SW Spain) over April 2008–December 2009 period (particle number, gaseous pollutants and black carbon concentrations and levels and chemical composition of PM$_{10}$ and PM$_{2.5}$ with daily and hourly resolution). This city is affected by emissions from the second largest Cu-smelter in Europe, phosphoric acid and fertilizer production plants and an oil refinery and petrochemical plant. Industrial emissions are the main cause of ultrafine particle episodes. When vehicle exhaust emissions are the main source, ultrafine particles typically show (24-h mean) concentrations within the range 14,700–5000 cm^{-3} (50th–1st), with 60% of these linked to this source and 30% to industrial emissions. In contrast, when daily mean levels of N are within the range 50,000–25,500 cm^{-3} (100th–70th), industrial and vehicle exhaust emissions accounted for 49 and 30%, respectively. High concentrations of toxic trace metals (As, Cu, Cd, Zn and Pb) were recorded when the study city suffered fumigations of the Cu-smelter plumes (e.g. 10–25 ng m^{-3} As, 1–2 ng m^{-3} Cd and >10^5 cm^{-3} of ultrafine particles). Because of these industrial emissions, ultrafine particle concentrations during daylight are about two times higher than those observed in other European cities. Recently, ultrafine particle emissions in vehicle exhausts have been subject to limit values in a recent stage of the EURO standards. Industrial emissions should also be considered.

© 2012 Elsevier Ltd. All rights reserved.

1. Introduction

Epidemiological studies performed during recent decades have shown that in urban areas there is a relationship between the mass concentration of particles smaller than 10 and 2.5 μm aerodynamic

* Corresponding author.
  E-mail address: rocio.fernandez@dgeo.uhu.es (R. Fernández-Camacho).

diameter (PM_{10} and $PM_{2.5}$, respectively) and cardiovascular and respiratory morbidity (WHO, 2005). Because of this, standards for PM_{10} and $PM_{2.5}$ have been set in many countries. More recent studies reveal that some of the cardiovascular effects attributed to exposure to $PM_{2.5}$ may be due to ultrafine particles (diameter smaller than 0.1 μm; Araujo & Nel, 2009). Ultrafine particles typically account for 80–90% of the total number concentrations and for <10% of the $PM_{2.5}$ particle mass concentration (Putaud et al., 2010 and references therein). Most of the $PM_{2.5}$ mass concentrations (≥90%) occur in the accumulation mode (0.1–1 μm). As a consequence ultrafine particles are not properly monitored using PM_{10} and $PM_{2.5}$ as air quality assessment metrics. The total number concentration of particles coarser than a given size (usually 2 or 10 nanometres) has been used as a metric representative of ultrafine particles (e.g. Puustinen et al., 2007). Size-resolved measurements have been used to study the sources and processes contributing to ultrafine particles (e.g. Casati et al., 2007). The correlation between particle number and $PM_{2.5}$ concentrations in urban ambient air is rather weak (Putaud et al., 2010). In urban areas it has been observed that organic matter and elemental carbon are the only two $PM_{2.5}$ components that may significantly correlate with the particle number, with this being attributed to vehicle exhaust emissions (Rodríguez et al., 2007). Because of the concern linked to ultrafine particle ambient air pollution, standards for particle number emissions have been set in EURO-5b (Regulation 692/2008).

Although biogenic SOA emissions may in general contribute to ultrafine and organic carbon concentrations, the high correlation between OC and BC in the study area points to anthropogenic emissions (industrial plus vehicle exhaust emissions) as dominant source. Particles emitted by this source tend to be bimodal, exhibiting a nucleation mode (<30 nm), constituted by sulphuric acid droplets that may be covered by condensed hydrocarbons, and a soot mode (50–200 nm; Kittelson, 1998). The formation rate of the nucleation mode particles is significantly influenced by ambient air conditions (e.g. wind speed, temperature and humidity; Casati et al., 2007). The soot mode is constituted by light-absorbing elemental carbon, primary organic carbon, condensed metals and sulphates and some carcinogenic organic pollutants (e.g. polycyclic aromatic hydrocarbons; Morawska and Zhang, 2002).

Up to the present date, modest attention has been paid to other potential major anthropogenic sources of ultrafine particles, even though it is well known that some activities may release large amounts of gaseous precursors. This is the case of some industrial activities that release large amounts of SO_2 and/or hydrocarbons. Sulphuric acid plays a key role in nucleation and new particle formation processes (Kulmala et al., 2004). These emissions result in gas-to-particle conversion processes that may prompt ultrafine and accumulation mode (0.1–1 μm) particle pollution. Nucleation of sulphur gases followed by particle growth by condensation and/or coagulation may result in the formation of ultrafine and fine particles and both (especially the latter) result in $PM_{2.5}$ pollution. These particles may be externally or internally mixed with trace elements linked to industrial emissions.

The development of techniques or methods for identifying the sources contributing to ultrafine particles is a major challenge in urban air quality nowadays. Several attempts have been made, by studying the relationship between particle number and $PM_{2.5}$ composition (Pey et al., 2009), by performing speciation of organic compounds (Kleeman et al., 2009) and by using the relationship between black carbon and particle number with a high time resolution (Rodríguez and Cuevas, 2007).

In this study we focused on identifying the sources and processes contributing to the number concentration of particles coarser than 2.5 nm in an urban area affected by industrial emissions. Different methods were used. Particle number concentrations were analysed using: 1) 1-h data of black carbon, trace gases and meteorological parameters measured over two years, 2) 1-h resolution data of $PM_{2.5}$ elemental composition, and 3) receptor-modelling techniques based on 2-years' data of 24-h average $PM_{2.5}$ chemical composition. Results show that the contribution of industrial emissions to ultrafine particles in the urban ambient air of industrial cities is comparable to that of vehicle exhausts.

2. Methodology

2.1. Study area

The study city (Huelva; 37°15′0″N, 6°57′0″W, 54 m.a.s.l) is located in SW Spain (Fig. 1). Air pollutants are mostly emitted by vehicle exhausts and by industrial activities in two estates to the south of Huelva: Punta del Sebo and Nuevo Puerto (Fig. 1). The second largest Cu-smelter factory in Europe (which emits SO_2, H_2SO_4, As, Sb, Pb, Zn and Sn) and a fertilizer and phosphoric acid production plant (which emits NH_4^+ and Na phosphate, phosphoric acid, sulphuric acid and sodium silicate) are located in Punta del Sebo. A crude oil refinery and a petrochemical complex (which
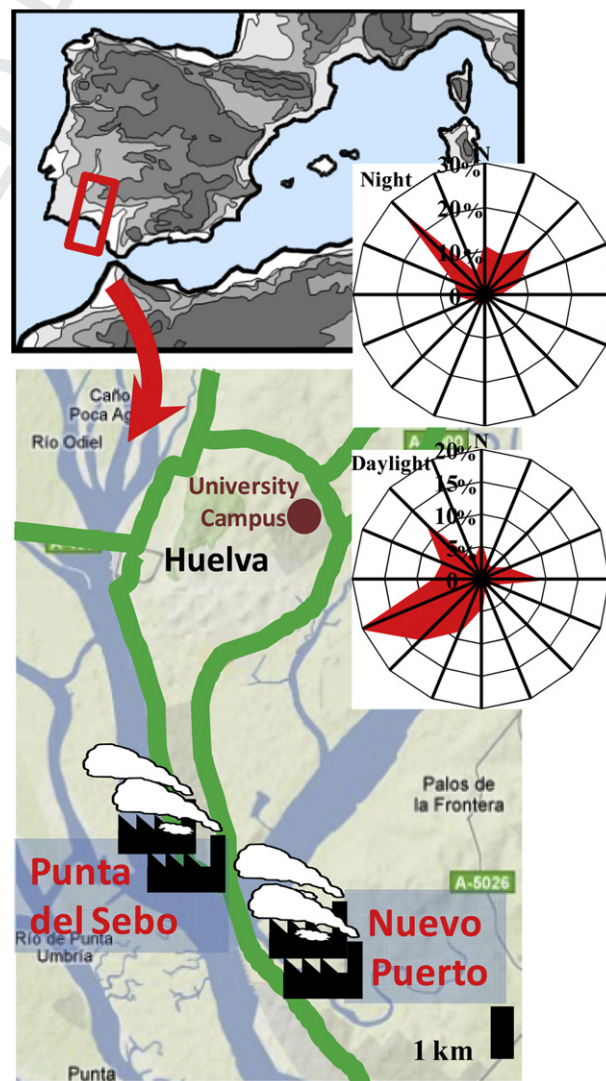

Fig. 1. Map of Huelva. Green lines indicate main roads and motorways around Huelva city. Punta del Sebo and Nuevo Puerto Industrial Estates and the University Campus measurement site are highlighted. (For interpretation of the references to colour in this figure legend, the reader is referred to the web version of this article.)

emits SO_2, NO_x, NH_3, Ni, V and a wide variety of hydrocarbons) are to be found in Nuevo Puerto. Pollutants emitted by these industries are described in previous works (De la Rosa et al., 2010; Fernández-Camacho et al., 2010a; Sánchez de la Campa et al., 2011) and in the European Pollution and Emission Register (http://eper.ec.europa.eu/eper/). These industrial emissions can reach the city of Huelva on the southerly winds episodically linked to specific synoptic conditions or on an almost daily basis linked to the development of coastal breezes during daylight (Castell et al., 2010).

2.2. Experimental data

Concentrations of gaseous pollutants and levels and composition of atmospheric particulate matter were monitored in an urban background station ($37°16'13.1''$, $6°55'30.9''$ m.a.s.l) located at the University Campus on the northern side of the city. The site is situated about 7 km from Punta del Sebo Estate and about 14 km from Nuevo Puerto Estate. Moreover, two entry roads to the city are located about 500 m to the west and about 1000 m to the east of the measurement site. The measurements used for this study were collected from April 2008 to December 2009.

2.2.1. Particle number, black carbon, PM_{10} and $PM_{2.5}$ concentrations

Details of the experimental methods have been presented by Fernández-Camacho et al. (2010b). Thus a brief summary is performed here. The particle number (PN) was monitored using a TSI™ 3776 model Ultrafine Condensation Particle Counter (UCPC). The instrument records data averaged at 1-min intervals and detects particles coarser than 2.5 nanometres (nm) operating in high-flow mode (1.5 l m^{-1}). Because 80–90% of particles in urban air are <0.1 μm, PN is considered representative of ultrafine particle number concentration. Black carbon (BC) concentration was monitored using a Thermo™ Carusso model 5012 Multi-Angle Absorption Photometer (MAAP). BC concentrations were calculated using a mass-specific attenuation cross-section equal to 10.31 m^2 g^{-1} (Fernández-Camacho et al., 2010b). Instruments were inter-compared before the measurement campaign and calibrated for airflow on a weekly basis using a Gilibrator™ bubble-flow meter. Data availability was 90% for BC and 70% for particle number.

PM_{10} and $PM_{2.5}$ were sampled (24-h) using EU reference methods: a Graseby Andersen™ sampler (68 m^3 h^{-1}, EN-12341) for PM_{10} and a MCV™ (30 m^3 h^{-1}, EN-14907) for $PM_{2.5}$. The sampling frequency was 1 sampling day (00:00–00:00 GMT) every four days in 2008 and every eight days in 2009. MUNKELL™ microquartz fibre filters were used. Filters were conditioned at 20 °C and 25% RH before weighting previous and after sampling. Blank field filters were also used.

Hourly levels of PM_{10} and $PM_{2.5}$ were monitored using a GRIMM™ optical particle counter. Their concentrations were converted to the gravimetric equivalent by comparing with the EU (gravimetric) reference method using the EU standardized method (EC Working Group on Particle Matter report, 2002).

2.2.2. Gaseous pollutants, meteorology and road traffic data

Concentrations of gaseous pollutants (SO_2, NO_x and O_3) were monitored with 1-h resolution using the reference methods of the European air quality directives (2008b/50/EC). Meteorological parameters (wind speed and direction, temperature, relative humidity, pressure and global radiation), monitored in a station less than 2 km away managed by the Meteorological State Agency (AEMET), and road traffic intensity data (number of vehicles h^{-1}), recorded on the two roads close to the measurement site, were also used. These data were obtained during 2008 and 2009 with 1-h resolution.

2.2.3. Bulk chemical composition of particles: 24-h resolution

Samples of PM_{10} and $PM_{2.5}$ collected on the microquartz fibre filters were chemically analysed using the method of Querol et al. (2008). This method includes ICP-OES and ICP-MS for elemental composition, Ion Chromatography for ions (SO_4^{2-}, NO_3^-, Cl^- and NH_4^+) and the LECO SC-144 DR instrument for total carbon. Average precision and accuracy are within the range of 3–10% for most elements and compounds. Silica and carbonate were estimated by stoichiometry using the Ca, Mg and Al data (Querol et al., 2001).

A set of 62 samples of PM_{10} and 59 samples of $PM_{2.5}$ were selected for the analysis of organic carbon (OC) and elemental carbon (EC), using the Thermo Optical Transmittance technique (Birch and Cary, 1996) and a Sunset Laboratory™ instrument with the default temperature steps of the EUSAAR2 program. The filters were selected in a homogeneous way, covering a representative range of concentrations of the area of study during the four seasons. The EC data were used to determine the mass-specific attenuation cross-section by comparison with the absorption coefficient measured by the MAAP. Then, mean black carbon (BC) concentrations were determined for each PM_{10} and $PM_{2.5}$ sample. To determine the BC load in $PM_{2.5}$, the mean ratio of BC in $PM_{2.5}$/BC in PM_{10} was used. A mass-absorption efficiency of 10.31 ± 0.25 m^2 g^{-1} and a mean BC in $PM_{2.5}$/BC in PM_{10} ratio equal to 0.74 ± 0.025 was obtained (see details in Fernández-Camacho et al., 2010b). Then, the organic carbon in each PM_{10} and $PM_{2.5}$ sample was determined as the difference between TC and BC. Finally, the organic matter was estimated by multiplying OC concentrations by 1.8 to take the contribution of other atoms into account (Turpin and Lim, 2001).

A total of 136 samples of PM_{10} and 134 samples of $PM_{2.5}$ collected from April 2008 to December 2009 were analysed using this method (Table 1).

2.2.4. Elemental composition of particles: 1-h resolution

A 'streaker' sampler (PIXE International Corporation) was employed to collect samples of fine (<2.5 μm aerodynamic diameter) and coarse (2.5–10 μm) particles with one hour resolution (D'Alessandro et al., 2003). A paraffin-coated kapton foil was used as an impaction surface for coarse particles and a Nuclepore filter as a fine particle collector. Elemental composition was determined by PIXE in the LABEC laboratory at INFN in Florence (Italy): Ti, V, Cr, Mn, Fe, Ni, Cu, Zn, As, Se, Sr and Pb as trace elements and Na, Mg, Al, Si, P, S, Cl, K and Ca as major elements. Concentration uncertainties were around 5%. Detection limits were about 10 ng m^{-3} for low-Z elements and 1 ng m^{-3} (or below) for medium-high Z elements. (Chiari et al., 2006). The sampling was performed from 15th to 22nd October 2009.

2.3. Data treatment

2.3.1. Components of ultrafine particles

In order to identify the sources and processes that contribute to the particle number concentrations, PN was split into two components (Rodríguez and Cuevas, 2007):

$$PN1 = S1 \cdot BC \tag{1}$$

$$PN2 = PN - PN1 \tag{2}$$

where S1 = 6.9 10^6 particlesng^{-1} BC is the minimum slope observed in the PN vs BC plot in our measurement site and represents the minimum number of particles formed/emitted per nanogram of BC emitted by vehicle exhausts (Fig. 2).

In cities where black carbon is dominated by vehicle exhaust emissions, this method allows to segregate the contribution of this source from that of other sources to the ultrafine particle

Table 1
Mean chemical composition of PM_{10} and $PM_{2.5}$ in Huelva from April 2008 to December 2009. NS: number of samples. OM: organic matter. SIC: secondary inorganic compounds.

NS	PM_{10}		$PM_{2.5}$		$PM_{2.5-10}$	
	136		134		134	
	µg m⁻³	%	µg m⁻³	%	µg m⁻³	%
PM	32.7 ± 13.0		19.3 ± 10.6		13.4 ± 8.0	
OM	5.8 ± 3.6	18	5.8 ± 3.6	30	0.0 ± 1.9	0
BC	0.8 ± 0.4	2	0.6 ± 0.4	3	0.2 ± 0.2	2
$nss-SO_4^{2-}$	3.0 ± 2.0	9	2.7 ± 1.6	14	0.3 ± 0.6	2
NO_3^-	2.6 ± 1.7	8	1.0 ± 1.1	5	1.6 ± 1.2	12
NH_4^+	0.8 ± 0.6	3	0.8 ± 0.7	4	0.0 ± 0.6	0
Na	1.3 ± 1.0	4	0.5 ± 0.3	3	0.8 ± 0.6	6
Cl^-	1.2 ± 1.4	4	0.2 ± 0.4	1	1.0 ± 1.1	7
$ss-SO_4^{2-}$	0.3 ± 0.2	1	0.1 ± 0.1	1	0.2 ± 0.2	1
$CO_3^=$	2.2 ± 1.2	7	0.8 ± 0.4	4	1.5 ± 1.0	11
SiO_2	4.6 ± 2.7	14	1.3 ± 0.8	6	3.3 ± 2.3	25
Al_2O_3	1.5 ± 0.9	5	0.4 ± 0.3	2	1.1 ± 0.8	8
Ca	1.0 ± 0.6	3	0.4 ± 0.2	2	0.7 ± 0.6	5
K	0.4 ± 0.2	1	0.2 ± 0.2	1	0.2 ± 0.1	1
Mg	0.3 ± 0.1	1	0.1 ± 0.1	0	0.2 ± 0.1	1
Fe	0.6 ± 0.3	2	0.2 ± 0.1	1	0.4 ± 0.3	3
PO_4^{3-}	0.2 ± 0.2	1	0.1 ± 0.1	0	0.1 ± 0.2	1
	ng m⁻³	‰	ng m⁻³	‰	ng m⁻³	‰
Ti	46.5 ± 30.1	1.4	17.8 ± 29.9	0.9	28.7 ± 25.0	2.1
V	5.3 ± 4.2	0.2	3.4 ± 3.2	0.2	1.9 ± 1.5	0.1
Cr	2.3 ± 2.0	0.1	1.6 ± 4.4	0.1	0.7 ± 1.8	0.1
Mn	9.6 ± 5.2	0.3	4.0 ± 2.0	0.2	5.6 ± 3.7	0.4
Co	0.3 ± 0.2	<0.1	0.2 ± 0.1	<0.1	0.1 ± 0.3	<0.1
Ni	3.7 ± 2.8	0.1	2.3 ± 1.7	0.1	1.4 ± 2.0	0.1
Cu	45.3 ± 30.2	1.4	31.2 ± 20.4	1.6	14.1 ± 17.5	1.1
Zn	47.4 ± 42.9	1.4	37.3 ± 49.5	1.9	10.1 ± 40.4	0.8
As	6.2 ± 7.8	0.2	5.1 ± 7.6	0.3	1.1 ± 4.1	0.1
Se	2.1 ± 2.8	0.1	1.7 ± 2.8	0.1	0.4 ± 1.6	<0.1
Rb	1.2 ± 0.7	<0.1	0.4 ± 0.4	<0.1	0.8 ± 0.5	0.1
Sr	6.2 ± 2.5	0.2	1.3 ± 0.7	0.1	4.9 ± 1.3	0.4
Mo	12.2 ± 1.6	0.4	0.7 ± 0.9	<0.1	11.5 ± 1.9	0.9
Cd	0.7 ± 0.9	0.0	0.6 ± 1.0	<0.1	0.1 ± 0.6	<0.1
Sn	2.6 ± 2.0	0.1	1.5 ± 1.3	0.1	1.1 ± 0.8	0.1
Sb	1.6 ± 0.9	<0.1	0.8 ± 0.6	<0.1	0.8 ± 0.5	0.1
Ba	31.9 ± 48.4	1.0	19.7 ± 36.7	1.0	12.2 ± 57.2	0.9
Pb	14.4 ± 15.2	0.4	10.8 ± 14.3	0.6	3.6 ± 4.3	0.3
Bi	0.9 ± 1.1	<0.1	0.8 ± 1.0	<0.1	0.1 ± 0.5	<0.1
	µg m⁻³	%	µg m⁻³	%	µg m⁻³	%
PM	32.7 ± 13.0		19.3 ± 10.6		13.4 ± 8.0	
∑ chemistry	26.9 ± 5.5	82.1	15.2 ± 3.3	78.5	11.7 ± 2.3	87.3
SIC	6.4 ± 1.2	19.6	4.5 ± 1.0	23.4	1.9 ± 0.8	14.2
OM	5.8 ± 3.6	17.8	5.8 ± 3.6	30.0	0.0 ± 1.9	0.2
BC	0.8 ± 0.4	2.5	0.6 ± 0.4	3.1	0.2 ± 0.2	1.5
Mineral dust	10.8 ± 1.4	32.9	3.3 ± 0.4	17.0	7.5 ± 1.0	55.9
Marine	2.9 ± 0.5	8.7	0.9 ± 0.2	4.4	2.0 ± 0.4	15.0

concentrations. PN1 accounts for the minimum primary emissions of vehicle exhausts and is constituted by the previously described soot mode (light-absorbing elemental carbon, carbonaceous material, trace metals, etc.) and those components nucleating and condensing immediately after emission (e.g. sulphates, condensed hydrocarbons and unburned oil). PN2 accounts for those particles resulting from enhancement in new particle formation processes in several contexts: during the dilution and cooling of vehicle exhausts or in ambient air linked to photochemical processes and/or in gas-to-particle conversion processes in precursor plumes. This method has successfully been applied in European cities (Reche et al., 2011).

2.3.2. Source apportionment

The sources that contribute to particle concentration were identified by performing Principal Component Analysis (PCA) followed by varimax rotation. Because the results of the PCA depend on the data set analysed, several combinations of variables were tested. The contribution of each source was quantified by Multi-
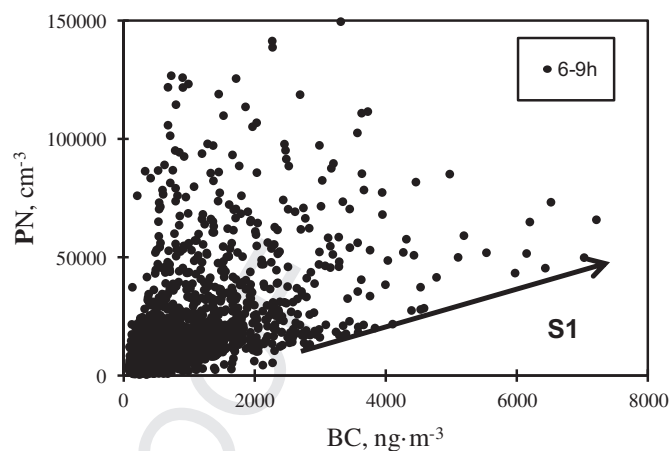

Fig. 2. Hourly average values of the particle number (PN) versus black carbon (BC) concentrations between 06:00 and 09:00 h. S1 indicates the line of minimum slope which contains N-vs.-BC data.

Linear Regression Analysis (Thurston and Spengler, 1985). The sources contributing to particle number were identified using the number concentration and $PM_{2.5}$ composition data. For PM_{10}, $PM_{2.5}$ and $PM_{2.5-10}$, bulk levels and composition data were analysed. Saharan events were excluded from the database in order to prevent the influence of external sources of sulphate, nitrate and other pollutants mixed with dust (Rodríguez et al., 2011).

3. Results and discussion

3.1. Chemical composition of particles

The mean chemical composition of PM_{10} and $PM_{2.5}$ is shown in Table 1. An average value equal to 32.7 ± 13 µg PM_{10} m⁻³ and 19.3 ± 11 µg $PM_{2.5}$ m⁻³ was observed. The most important contributors to $PM_{2.5}$ were secondary inorganic compounds (sulphate, nitrate and ammonium) and organic matter, which accounted for 23% and 30% of $PM_{2.5}$, respectively. The sulphate load was large, accounting for 14% of $PM_{2.5}$. Because these compounds mostly occur in the <2.5 µm fraction, their absolute concentrations in PM_{10} and $PM_{2.5}$ are close. As expected, the mineral dust and sea salt mostly occur in the coarse 2.5–10 µm fraction. The mean contribution of major species to PM_{10} and $PM_{2.5}$ is similar to that observed in other cities in Spain (Querol et al., 2004a, 2008). The most significant feature of the PM_{10} and $PM_{2.5}$ composition in Huelva is the high content of toxic trace metals of environmental interest. Concentrations of As, Cu, Zn, Se and Bi are 3–5 times higher than those typically observed in other European cities (Querol et al., 2004b, 2008; Rodríguez et al., 2007; Putaud et al., 2004). Mean concentration of As (6.2 ng m⁻³) is slightly higher than the annual target value of the European standard (6 ng m⁻³ in PM_{10}; 2004/107/EC).

3.2. Influence of industrial emissions on composition and daily evolution of particles

3.2.1. Ultrafine particles and gaseous pollutants

Figure 3 shows the hourly average values for particle number (PN, PN1 and PN2), BC concentrations and gaseous pollutant concentrations, road traffic intensity, road traffic intensity/wind speed and some meteorological parameters and $PM_{2.5}$ and $PM_{2.5-10}$ concentrations. Working days (Monday to Friday) and weekends are segregated. The influence of vehicle exhaust and industrial emissions on the particle number concentration tends to occur at
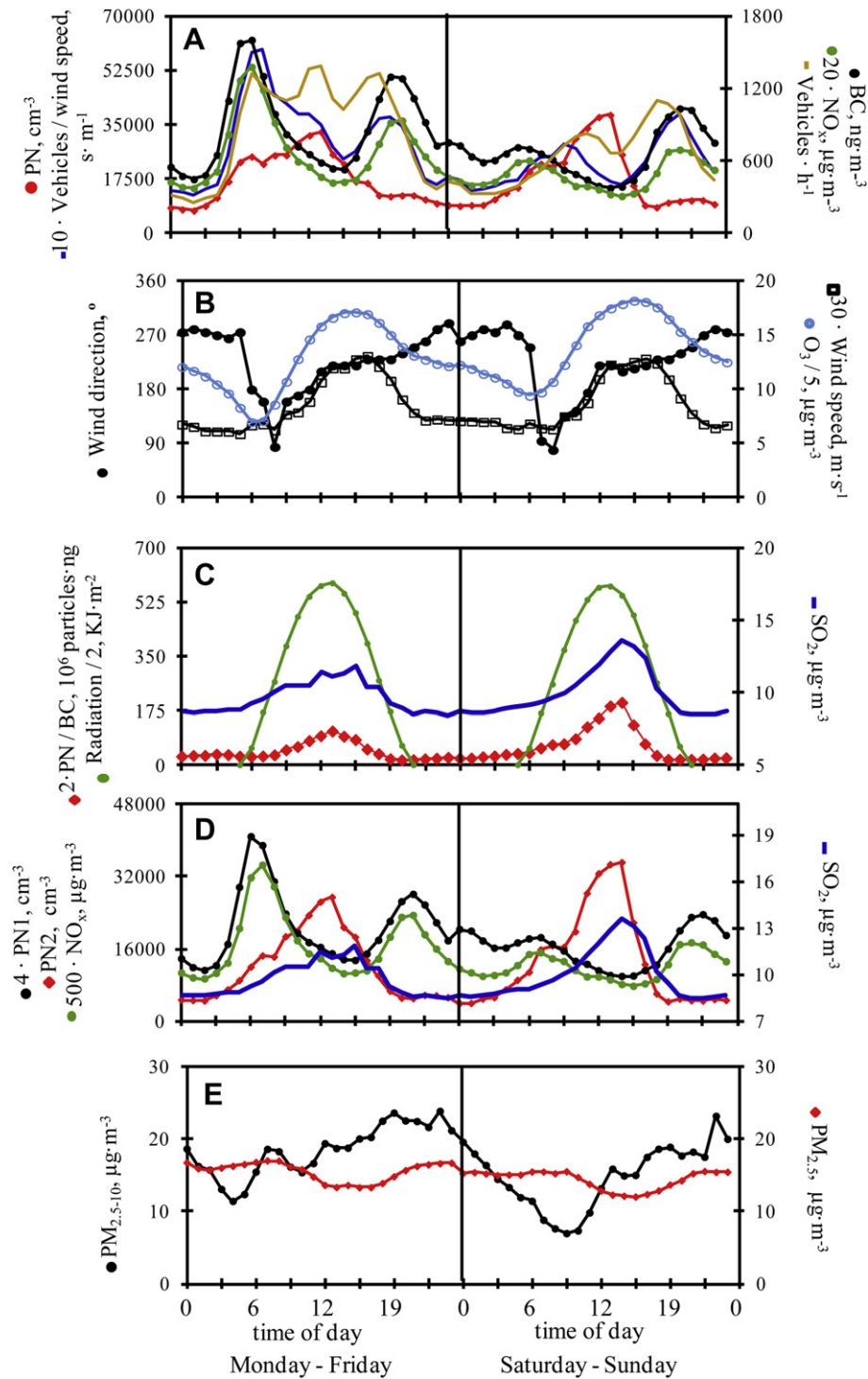
Fig. 3. Hourly average values of particles (PN, PN1 and PN2), BC concentrations and gaseous pollutant (NO$_x$ and SO$_2$) concentrations, and of road traffic intensity, the road traffic intensity (number of vehicles/h)/wind speed ratio, of the PN/BC ratio and solar radiation and of PM$_{2.5}$ and PM$_{2.5-10}$ concentrations, for working days, Saturdays and Sundays during 2008–2009.

different times of day. The sharp increase in road traffic intensity in the morning results in an abrupt rise in PN, BC and NO$_x$ concentrations due to vehicle exhaust emissions. The enhancement in the dilution conditions and air mass renewal due to the development of inland sea breeze after 09:00 GMT, results in a decrease in the concentration of these vehicles exhaust pollutants, even if the road traffic intensity does not decrease. The correlated weekly evolution of road traffic intensity / wind speed ratio and BC and NO$_x$

concentrations indicates that fresh vehicle exhaust emissions and dilution/ventilation conditions modulate the behaviour of these pollutants (Fig. 3A).

The inland sea breeze blowing from 09:00 to 17:00 GMT is associated with an increase in the sulphur dioxide concentrations (Fig. 3B and C). This is attributed to the inland transport of plumes from the industrial estates located to the south of Huelva (Fig. 1). Observe the correlation between the daily evolution of SO$_2$, wind

speed and solar radiation. The increase in the PN/BC ratio and in PN2 concentrations observed during the inland blowing period is attributed to ultrafine particle formation in the SO_2 plumes. Fernández-Camacho et al. (2010b) showed that there is a strong statistical relationship between PN2 and SO_2, and between PN1 and NO_x, in such a way that PN2 tends to show high values during fumigations of industrial plumes, whereas PN1 shows high values linked to vehicle exhaust emissions. Stanier et al. (2004) and Cheung et al. (2011) observed that high particle number concentration in industrial SO_2 plumes was due to nucleation burst linked to the sulphuric acid/sulphate particles. During the morning NO_x maximum period, when ultrafine particles were linked to vehicle exhaust emissions, PN is higher on average value than 23,000 cm^{-3}, and PN2 accounted for 53% of PN, whereas during the noon − afternoon SO_2 maximum due to the impact of the industrial plumes, PN is typically higher on average value than 29,000 cm^{-3}, and PN2 accounted for 70% of PN.

3.2.2. Ultrafine particles and elemental composition

The mean daily evolution (hourly values) of PN, SO_2 and NO_x and of $PM_{2.5}$ elemental composition observed during the weekdays (Monday to Friday) and weekends (Saturday and Sunday) of the streaker campaign (15th to 22nd October 2009) is shown in Figure 4. The two types of ultrafine particle episodes are recognized:

- *Fresh road traffic emissions.* These are observed during the morning rush hours of the working days and are associated with high concentrations of typical road dust elements (Si, Al, Fe, Mg, K, Ca, Ti and Mn; Amato et al., 2009).
- *Fresh industrial plumes.* These events are associated with high concentrations of trace metals (As, Cu, Zn, Se, Pb and P) during the central hours of daylight (10:00−17:00 GMT) due to inland transport of the industrial plumes both during weekdays and weekends. The Fig. 4B shows the highest concentrations of PN, trace metals and SO_2 occurring during weekends. This fact can probably be due to the work regime of industrial estates, as during weekends and holidays, the electric cost is cheaper (by 60−70%).

The occurrence of high PN and trace metal concentrations due to the impact of the industrial plumes (containing SO_2) is clearly observed in Figure 5A. Observe that several events of N and As concentrations as high as 10^5 cm^{-3} and 18 ng m^{-3} occurred during the streaker campaign. Because the stacks of the Cu-smelter and fertilizer plants are very close together in Punta del Sebo Estate (Fig. 1), simultaneous high As and P events occurred due to mixing of the plumes during inland transport.

The hourly evolution of S (in $PM_{2.5}$) and bulk $PM_{2.5}$ is compared with that of N and Zn (in $PM_{2.5}$) in Fig. 5B. It can clearly be observed that the $PM_{2.5}$ and S concentrations do not properly detect the fumigations of the industrial plumes. Only in the fumigations that occurred on 18th October is an increase in S concentrations observed. Moreover, high S and bulk $PM_{2.5}$ concentrations were observed during periods of non-fumigation or fresh emissions, e.g. 17th October at night. This indicates that S and $PM_{2.5}$ concentrations are linked to aged emissions, i.e. they are aged grown particles occurring in the accumulation mode (0.1−1 μm). In contrast, the high PN and SO_2 concentrations are attributed to fresh ultrafine sulphuric acid/sulphate formation in the industrial plumes (Fig. 5A). The contribution of this ultrafine sulphuric acid/sulphate to bulk S (in $PM_{2.5}$) is so low that it does not result in significant increases in the concentration of the S (Fig. 5B). Similar behaviour was identified in Milan (Italy) and Barcelona (Spain) by Rodríguez et al. (2007); they observed that high $PM_{2.5}$ concentrations were associated with particle growth due to condensation of ammonium nitrate and ammonium sulphate in aged air, whereas fresh emissions resulted in much larger increases in ultrafine than in $PM_{2.5}$ particles. The streaker data showed that S, V, Ni, Cr and Br did not show a daily pattern, and high concentrations of these elements were recorded linked to specific events.

Observe in Fig. 5C how PN exhibits a high correlation with elements linked to the fresh industrial Cu-smelter emissions (e.g. Zn, Cu and Pb, r: 0.48−0.64) and the phosphoric acid-based fertilizer plant (e.g. P, r = 0.44). In contrast, $PM_{2.5}$ shows high correlation with compounds linked to aged emissions from the oil refinery (S, V and Ni; r: 0.4−0.6) and road dust (Fe, Ca, K, Al and Sr; r: 0.3−0.4).
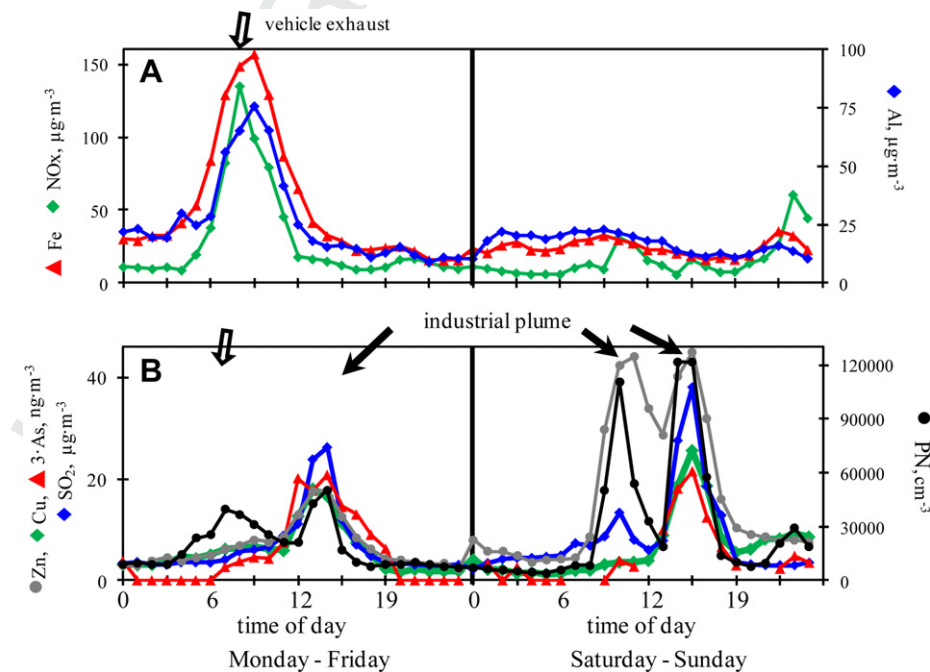

Fig. 4. Daily evolution (hourly values) of particle number (PN), gaseous pollutants (NO_x and SO_2) and Fe, Al, Zn, Cu and As in $PM_{2.5}$ averaged during weekdays (Monday−Friday) and weekends (Saturday−Sunday) of the streaker campaign.
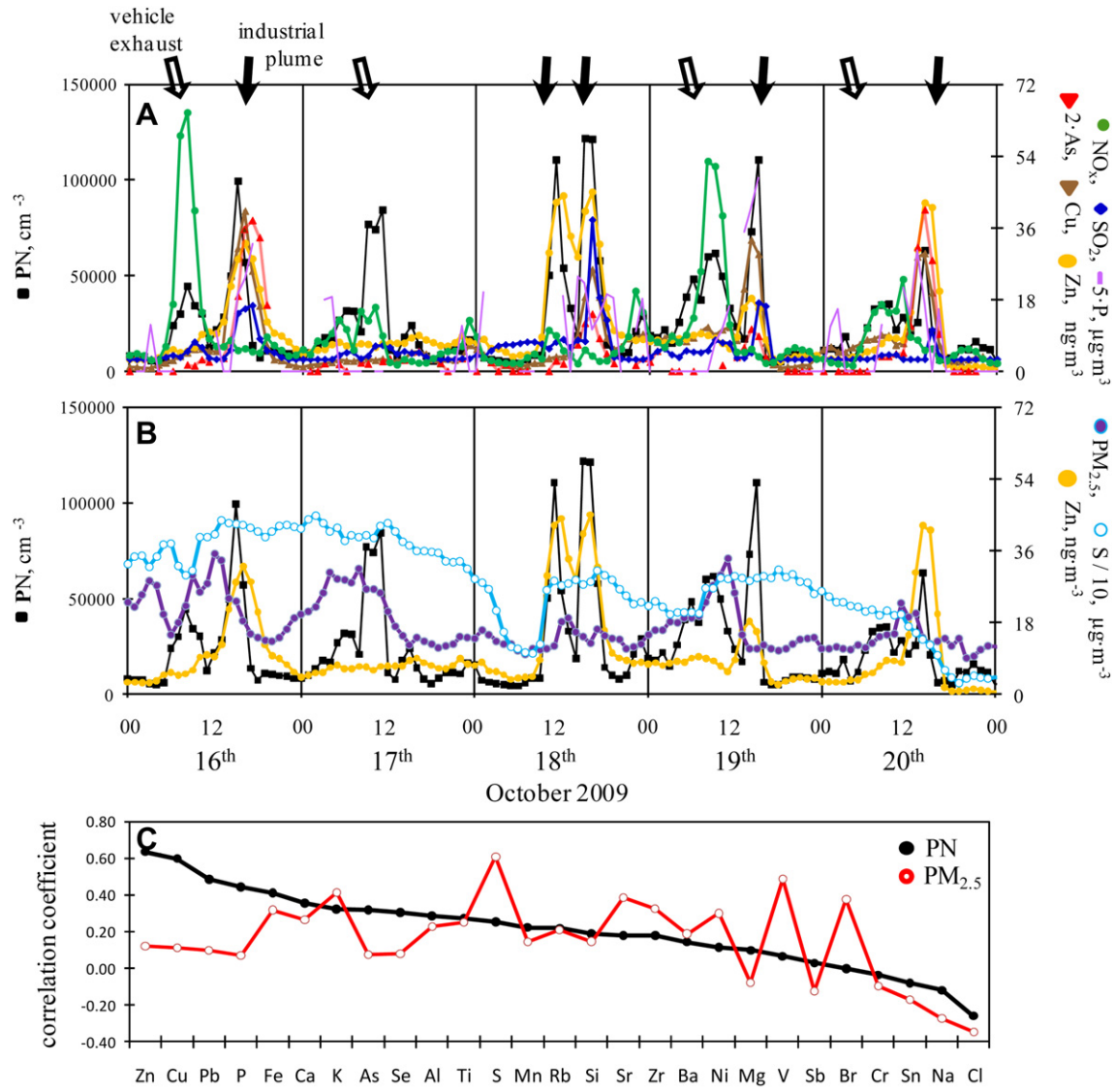
7

Fig. 5. A–B) Hourly average values of particle number (PN), SO$_2$, NO$_x$, some trace metals (P, As, Cu and Zn) and sulphur (S) in PM$_{2.5}$. C) Correlation coefficient between PN and all the elements analysed in PM$_{2.5}$. All data have hourly time resolution. Scale factor has been applied for some elements (x 2 for As, x 5 for P, /10 for S) in order to adjust the scale of the graphic.

3.3. Ultrafine particles episodes

A classification of ultrafine particle events was performed. This was done by identifying the pollutants that tend to increase simultaneously with hourly particle number concentration N. This classification allows the most frequent scenarios in which ultrafine particle events occur to be identified. Eight types of event, in which N experiences simultaneous increases with NO$_x$, SO$_2$, BC and/or solar radiation, were considered (Table 2). The most frequent time of occurrence and mean concentrations of the measured parameters are included in the analysis. The overall results show that:

- 29% of the peak events in hourly PN concentrations occurred in the morning (08:00 GMT) with concurrent increase of NO$_x$ and BC concentrations. These type-1 events are attributed to vehicle exhaust emissions.
- 31% of the peak events in PN were simultaneous with increases in SO$_2$ concentrations (type 2, 4, 6 and 8). Most of

these events occurred from 13:00 to 14:00 GMT, when industrial plumes typically reach the measurement site. In most of these events (21% of all PN increases) NO$_x$ was the only pollutant that experienced a simultaneous increase with SO$_2$ and PN (type-6).

- In ~20% of the events, no increase in the measured pollutants was observed during the increases in PN concentrations. These type-3 events mostly occurred at noon, when simultaneous increases in PN and in solar radiation were observed.

Fig. 6A and B show the mean PN versus SO$_2$ and O$_3$ concentrations recorded in all types of events (data included in Table 2). It can clearly be observed how particle number tends to increase with SO$_2$ and O$_3$ concentrations. In fact, the highest PN concentrations are recorded during type-6 ($N = 80,891$ cm^{-3}) events, which are associated with the highest SO$_2$ (28 μg m^{-3}) and O$_3$ (98 μg m^{-3}) concentrations. This result suggests the significant involvement of photochemistry in the processes involved in the

Table 2
Classification of ultrafine particle events. Type, characteristic, frequency, most frequent time of occurrence (GMT), and concentrations of the considered pollutants.

Type of events	PN peak correlated with	F	Time	PN cm^{-3}	PN1 %	PN2 %	NO$_x$ µg m^{-3}	SO$_2$ µg m^{-3}	BC ng m^{-3}	O$_3$ µg m^{-3}
NO$_x$ involved		**36%**								
Type-1	NO$_x$ and BC	29%	8:00	22,352	37	63	52	8	1351	50
Type-5	NO$_x$	7%	13:00	45,989	7	93	33	8	497	74
SO$_2$ involved		**31%**								
Type-2	SO$_2$, BC and NO$_x$	5%	13:00	33,828	16	84	30	20	807	81
Type-4	SO$_2$	4%	14:00	71,989	6	94	20	25	622	82
Type-6	SO$_2$ and NO$_x$	21%	13:30	80,891	5	95	32	28	608	98
Type-8	SO$_2$ and BC	1%	11:00	23,466	14	86	6	12	472	75
Only BC involved		**14%**								
Type-7	BC	14%	11:00	18,080	20	80	18	7	603	69
Non primary pollutants		**20%**								
Type-3	Only solar radiation	20%	12:00	36,994	9	91	20	9	505	76

conversion of SO$_2$ to ultrafine particles within the industrial plumes during inland transport prompted by sea breeze. Observe how the PN2 contribution to PN increases with O$_3$ concentrations (Fig. 6D). The contribution of PN1 to PN is only significant during type-1 events (primary vehicle exhaust emissions), when it reaches 37% (Table 2). The contribution of PN2 particles to PN is also high during type-3 and 5 events, even if SO$_2$ concentrations are rather low (8—9 µg m^{-3}). The relationship between PN2 and O$_3$ during these events (a linear trend similar to that observed in all events) suggests the involvement of photochemical processes (Fig. 6D). The fact that increases in SO$_2$ concentrations were not observed in these events could be due to the fact that SO$_2$ is consumed by conversion to sulphate, or species other than SO$_2$ are involved in the nucleation and subsequent particle growth (e.g. organic species; Metzger et al., 2010; Sipilä et al., 2010).

3.4. Sources that contribute to ultrafine particles

The sources that contribute to ultrafine particles were identified by applying PCA and varimax rotations to data for particle number concentration data and PM$_{2.5}$ chemical composition. Different

combinations of variables were tested (e.g. PN and PM$_{2.5}$ composition, PN1, PN2 and PM$_{2.5}$ composition, including trace gases and/or meteorological parameters). A PCA with 45 cases and 27 variables was considered using the software package STATISTICA 7. Three Principal Components (PCs) were persistently observed (Table 3):

- APC-1, showing a high association with species linked to industrial emissions from the Cu-smelter (nss-SO$_4^=$, As, Sb, Pb, Zn and Sn), the phosphoric acid and fertilizer plant (nss-SO$_4^=$, P and NH$_4^+$) and the oil refinery (nss-SO$_4^=$, NO$_3^-$, NH$_4^+$, V and Ni), was persistently observed. The presence of PN2 in this PC is attributed to ultrafine sulphate particle formation in the plume during inland transport prompted by sea breeze. The association of PN2 in this factor is in agreement with the results above obtained using the streaker, which showed high concentrations of PN and trace metals during fumigations of the industrial SO$_2$ plumes (Figs. 4B and 5A).
- APC-2 associated with road traffic emissions: vehicle exhaust emissions (OM and PN1) plus road dust (Al, Ca, Fe, Ti, Mn and K). The association of this PC with particle number (PN1) is due to vehicle exhaust emissions, with the contribution of road
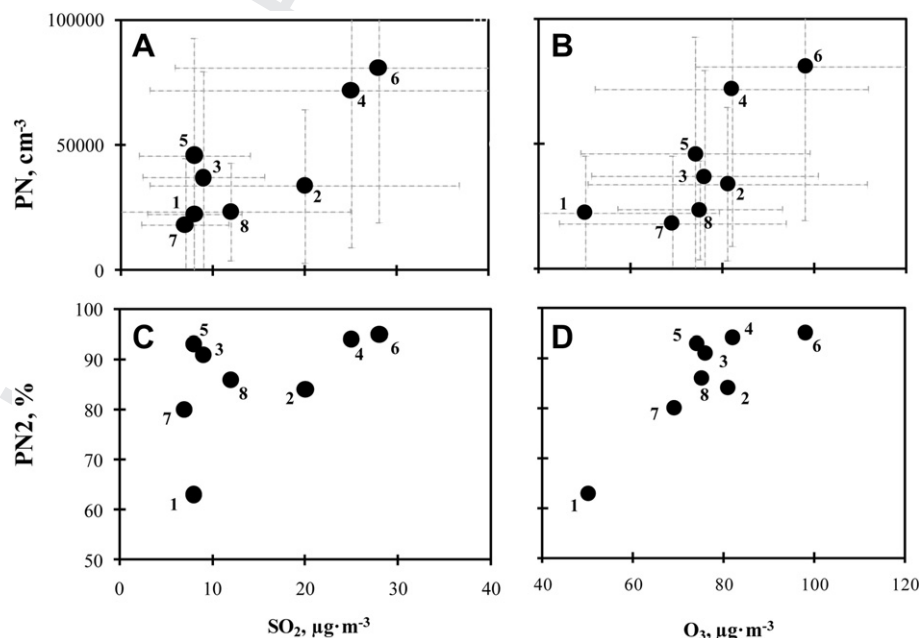

Fig. 6. Contributions of PN in absolute concentrations (cm^{-3}; A and B) and of PN2 in relative concentrations (%, C and D) versus SO$_2$ and O$_3$ concentrations. The number near each dot indicates the type of event described in Table 2. A and B) Dotted lines indicate plus/minus one standard deviation.

Table 3
Factor loading of the Principal Components Analysis (followed by a varimax rotation) obtained using daily data of $PM_{2.5}$ chemical composition and of PN1 and PN2 particles.

	PC-1	PC-2	PC-3
	Industrial	Road traffic	Sea salt
OM	0.37	**0.57**	−0.10
PN1	0.52	**0.59**	−0.10
PN2	**0.57**	0.26	−0.06
nss-SO_4^{2-}	**0.84**	−0.02	−0.14
NO_3^-	0.51	0.26	−0.14
NH_4^+	**0.87**	0.05	−0.29
Na	−0.08	−0.06	**0.86**
Cl^-	0.15	−0.03	**0.81**
Mg	−0.13	0.33	**0.83**
Al	0.13	**0.76**	−0.21
Ca	−0.07	**0.89**	0.14
Fe	0.14	**0.95**	0.05
Ti	0.14	0.46	0.25
Mn	0.26	**0.83**	0.12
K	0.29	**0.71**	0.13
P	**0.67**	0.10	0.10
As	**0.83**	0.26	0.16
Pb	**0.86**	0.21	0.28
Cd	**0.88**	0.18	0.32
V	**0.82**	0.25	−0.09
Ni	**0.74**	0.29	0.02
Zn	**0.61**	0.11	0.31
Cu	0.44	0.13	−0.05
Bi	**0.81**	0.07	0.39
Mo	0.53	−0.01	0.21
Sn	**0.71**	0.44	0.20
Sb	0.41	0.30	−0.29
% Var	39.20	12.00	11.70

dust considered being almost negligible (road dust is mostly coarse, with a high contribution to mass, but a low contribution to number concentrations). The association of road dust in this PC is attributed to the simultaneous (correlated) increases in road dust and vehicle exhaust components during the morning rush hours (e.g. Fig. 4A). The presence of PN1 in this PC is in agreement with the weekly cycles of NO_x and PN1 particles described above, which exhibited high values during working-day rush hours (Fig. 3).

- APC-3 showing high factor loading for typical sea salt components (Cl, Na and Mg). As expected, neither of the particle number components, PN1 or PN2, was associated with this factor.

Only two sources contributed significantly to the particle number PN: road traffic accounted for $50 \pm 9\%$, whereas industrial emissions accounted for $44 \pm 7\%$ of PN (Fig. 7). The contribution of sea salt was negligible (<1%), whereas the undetermined fraction (the difference between measured PN and the sum of the identified sources) accounted for 4% (Fig. 7). The contribution of these two
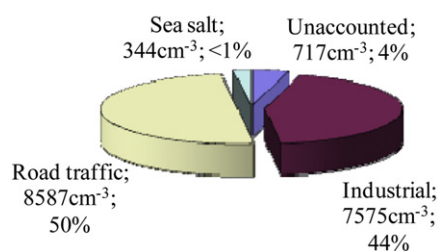
Mean contribution to PN (16536 cm⁻³)

Sea salt; 344cm⁻³; <1%
Unaccounted; 717cm⁻³; 4%
Road traffic; 8587cm⁻³; 50%
Industrial; 7575cm⁻³; 44%

Fig. 7. Mean daily contribution to PN (cm^{-3} and %) of the different factors identified by the PCA analysis.
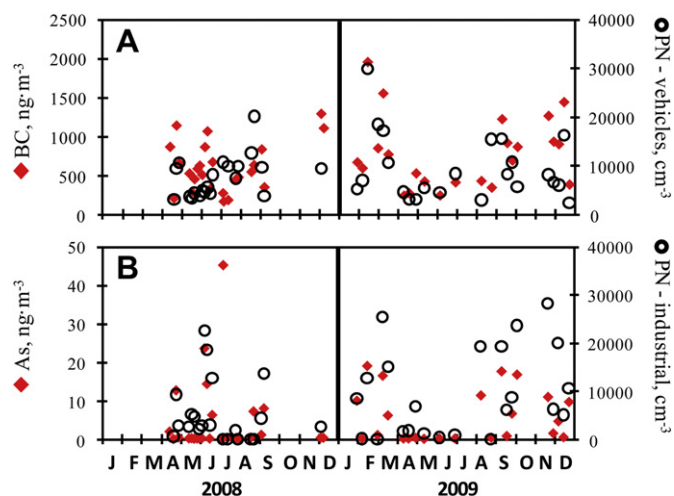
Fig. 8. Daily averaged values of BC, As and of the particle number PN linked to vehicle exhaust and industrial emissions.

sources to ultrafine particle concentration in ambient air is of a comparable magnitude: the daily mean contribution of each of these sources to the particle number concentration exhibits values within the range $10{,}000–30{,}000$ cm^{-3} (Fig. 8). Observe how industrial emissions can frequently contribute $20{,}000–30{,}000$ cm^{-3} to the particle number and can result in As concentrations within the range $10–25$ ng m^{-3} (Fig. 8B). Fig. 9 shows the daily mean
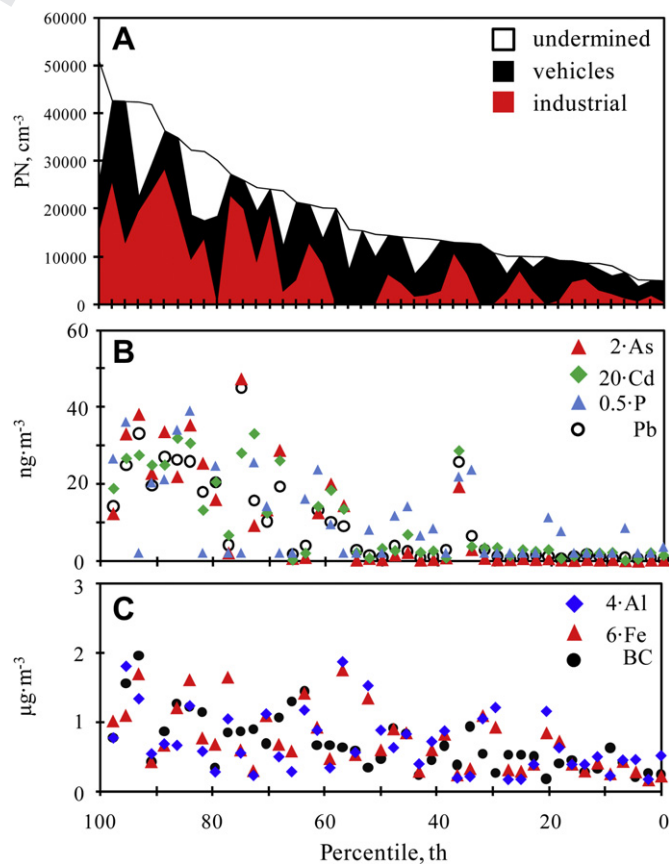
Fig. 9. A) Daily averaged values of PN classified from the highest to the lowest concentration (100th to 1st percentile) highlighting the contribution of the industrial, vehicle exhaust and undetermined fraction contributions. The associated concentrations of As, Cd, P, Pb, Al, Fe and BC are plotted in B and C.

averaged values of the particle number PN, classified from the highest to the lowest concentration (100th to 1st percentile), and the contribution of the identified sources. Observe how PN values $>25,500$ cm^{-3} (70th P) are mainly induced by industrial emissions, whereas for PN values $<14,700$ cm^{-3} (50th P) the vehicle exhaust contribution is greater:

- For daily mean levels of PN within the range 50,000–25,500 cm^{-3} (100th–70th) industrial and vehicle exhaust emissions accounted for 49 and 30%, respectively.
- For daily PN values within the range 14,700–5000 cm^{-3} (50th–1st), vehicle emissions accounted for 60% of PN, with only 30% of PN being linked to industrial emissions.

These results suggest that high PN concentrations, about 25,000 cm^{-3}, are mostly due to industrial emissions. Observe the sharp increase in the concentrations of As, Cd, Pb and P (linked to the Cu-smelter and fertilizer production plants) when PN concentrations higher than the 70th P are recorded (Fig. 9B). In contrast, compounds linked to vehicle exhaust and road dust emissions increase progressively from low to high PN events (Fig. 9C).

The potential contribution of new particle formation in ambient air linked to photochemical processes, typically occurring with low concentrations of primary pollutants (e.g. NO$_x$ and SO$_2$; Rodríguez
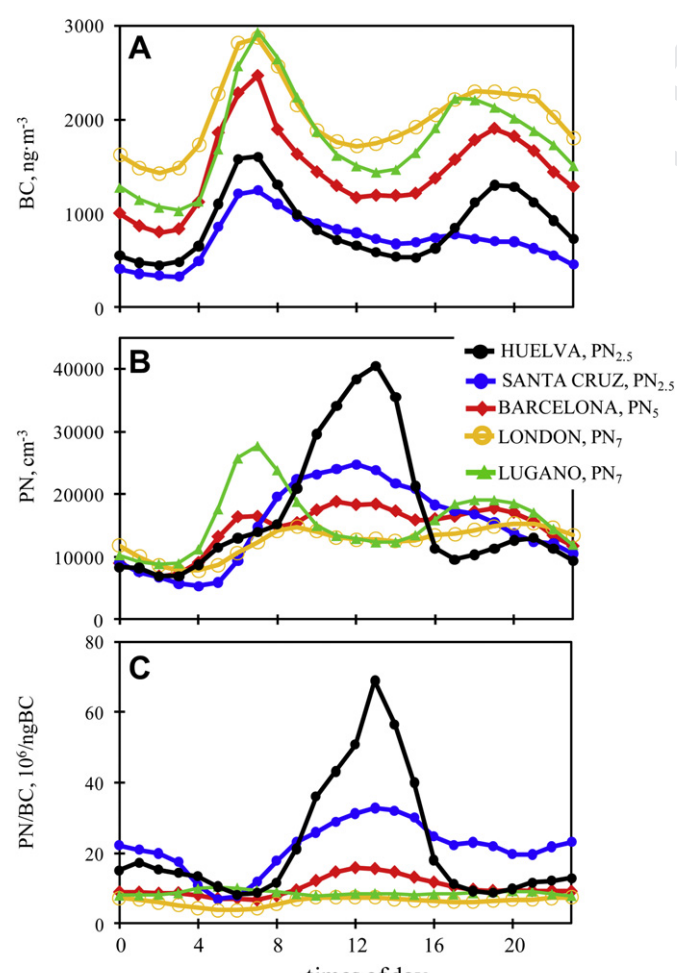

Fig. 10. Daily evolution of black carbon (BC), particle number (PN) and the number to black carbon ratio (PN/BC) in several European cities. PN$_x$: number concentrations of particles with a size higher than x nanometers. Data from Santa Cruz (Spain), Barcelona (Spain), London (UK) and Lugano (Switzerland) provided by Reche et al. (2011).

et al., 2009), was not identified in our PCA, with this being attributed to the fact that any chemical tracer of such a process was analysed. The features of the type-3 events we observed in the time series analysis suggest that these events occur in our study area. In fact, these events could account for the unexplained variance in the PCA ($\sim$37%) and for the unaccounted-for fraction in the source contribution (4%; Fig. 7). Pey et al. (2009) identified such photochemically induced new particle formation events in Barcelona, and concluded that they accounted for 3% of the number of particles >10 nm and for 23% of 10–20 nm particles.

The high impact of these industrial emissions on the ultrafine particle concentration is clearly observed in Fig. 10, where the number and black carbon concentration in several European cities is plotted (Reche et al., 2011). In Huelva, BC concentrations exhibit a maximum during the morning rush hours, as in other EU cities due to the dominant role of vehicle exhaust emissions. However, the particle number concentration in Huelva shows a distinct maximum during the noon–afternoon due to the impact of the industrial plumes over the city. Because of this, PN concentrations in Huelva are much higher than in other cities, even though BC levels in Huelva are significantly lower.

4. Conclusions

Urban air pollution by ultrafine particles is a matter of concern due to the adverse effects on human health. Studies performed during the last decade showed that vehicle exhausts are a major source of ultrafine particles in urban ambient air. Thus, ultrafine particle emissions in vehicle exhaust have recently been subject to limit values in a recent stage of the EURO standards.

The results of this study show that some industrial emissions result in high concentrations of ultrafine particles. This is the case of the industrial city of Huelva, where the second largest Cu-smelter plant in Europe, phosphoric acid and fertilizer plants, an oil refinery and a petrochemical plant are located. These sources release SO$_2$, toxic metals and hydrocarbons, among other pollutants. The results of this study show that industrial emissions are the main cause of ultrafine particle episodes. When vehicle exhaust is the main source, ultrafine particles typically show (24-h mean) concentrations within the range 14,700–5000 cm^{-3} (50th–1st), with 60% of these being linked to this source and 30% to industrial emissions. In contrast, when daily mean levels of PN are within the range 50,000–25,500 cm^{-3} (100th–70th), industrial and vehicle exhaust emissions accounted for 49 and 30%, respectively. High concentrations of toxic trace metals (As, Cu, Cd, Zn and Pb) are recorded during these ultrafine particle pollution events linked to industrial emissions (e.g. 10–25 ng m^{-3} As and 1–2 ng m^{-3} Cd). Because of these industrial emissions, ultrafine particle concentrations during daylight are about two times higher than those observed in other European cities.

References

Amato, F., Pandolfi, M., Escrig, A., Querol, X., Alastuey, A., Pey, J., Perez, N., Hopke, P.K., 2009. Quantifying road dust resuspension in urban environment by Multilinear Engine: a comparison with PMF2. Atmospheric Environment 43, 2770—2780.

Araujo, J.A., Nel, A.E., 2009. Particulate matter and atherosclerosis: role of particle size, composition and oxidative stress. Particle and Fibre Toxicology 6, 24. http://dx.doi.org/10.1186/1743-8977-6-24.

Birch, M.E., Cary, R.A., 1996. Elemental carbon-based method for monitoring occupational exposures to particulate diesel exhaust. Aerosol Science and Technology 25, 221—241.

Casati, R., Scheer, V., Vogt, R., Benter, T., 2007. Measurement of nucleation and soot mode particle emission from a diesel passenger car in real world and laboratory in situ dilution. Atmospheric Environment 41, 2125—2135.

Castell, N., Mantilla, E., Salvador, R., Stein, A.F., Millán, M., 2010. Photochemical model evaluation of the surface ozone impact of a power plant in a heavily industrialized area of southwestern Spain. Journal of Environmental Management 91, 662—676.

Cheung, K., Daher, N., Kam, W., Shafer, M.M., Ning, Z., Schauer, J.J., Sioutas, C., 2011. Spatial and temporal variation of chemical composition and mass closure of ambient coarse particulate matter ($PM_{10-2.5}$) in the Los Angeles area. Atmospheric Environment 45, 2651—2662.

Chiari, M., Del Carmine, P., Garcia Orellana, I., Lucarelli, F., Nava, S., Paperetti, L., 2006. Hourly elemental composition and source identification of fine and coarse PM10 in an Italian urban area stressed by many industrial activities. Nuclear Instruments & Methods in Physics Research Section B-Beam Interactions with Materials and Atoms 249, 584—587.

D'Alessandro, A., Lucarelli, F., Mandò, P.A., Marcazzan, G., Nava, S., Prati, P., Valli, G., Vecchi, R., Zucchiatti, A., 2003. Hourly elemental composition and sources identification of fine and coarse PM10 particulate matter in four Italian towns. Journal of Aerosol Science 34 (2), 243—259.

De la Rosa, J.D., Sánchez de la Campa, A.M., Alastuey, A., Querol, X., González-Castanedo, Y., Fernández-Camacho, R., Stein, A.F., 2010. Using PM10 geochemical maps for defining the origin of atmospheric pollution in Andalusia (Southern Spain). Atmospheric Environment 44, 4595—4605.

EC Working group on particulate matter, January 2002. REPORT — Guidance to Member States on PM10 Monitoring and Intercomparisons with the Reference Method.

EU, 2008a. Commission Regulation (EC) No 692/2008. Official Journal of the European Union 136.

EU, 2004. 2004/107/CE. Council Directive Relating to Arsenic, Cadmium, Mercury, Nickel and Polycyclic Aromatic Hydrocarbons in Ambient Air. The Council of the European Union.

EU, 2008b. 2008/50/EC Council Directive on ambient air quality and cleaner air for Europe. Official Journal L 152, 0001—0044.

Fernández-Camacho, R., de la Rosa, J., Sánchez de la Campa, A.M., González-Castanedo, Y., Alastuey, A., Querol, X., Rodríguez, S., 2010a. Geochemical characterization of Cu-smelter emission plumes with impact in an urban area of SW Spain. Atmospheric Research 96, 590—601.

Fernández-Camacho, R., Rodríguez, S., de la Rosa, J., Sánchez de la Campa, A.M., Viana, M., Alastuey, A., Querol, X., 2010b. Ultrafine particle formation in the inland sea breeze airflow in Southwest Europe. Atmospheric Chemistry and Physics 10, 9615—9630.

Kittelson, D.B., 1998. Engines and nanoparticles: a review. Journal of Aerosol Science 29, 575—588.

Kleeman, M.J., Riddle, S.G., Robert, M.A., Jakober, C.A., Fine, P.M., Hays, M.D., Schauer, J.J., Hannigan, M.P., 2009. Source apportionment of fine ($PM_{1.8}$) and ultrafine ($PM_{0.1}$) airborne particulate matter during a severe winter pollution episode. Environmental Science and Technology 43 (2), 272—279.

Kulmala, M., Vehkamäki, H., Petäjä, T., Dal Maso, M., Lauri, A., Kerminen, V.-M., Birmili, W., McMurry, P.H., 2004. Formation and growth rates of ultrafine atmospheric particles: a review of observations. Journal of Aerosol Science 35 (2), 143—176.

Metzger, A., Verheggen, B., Dommen, J., Duplissy, J., Prévôt, A.S.H., Weingartner, E., Riipinen, I., Kulmala, M., Spracklen, D.V., Carslaw, K.S., Baltensperger, U., 2010. Evidence for the role of organics in aerosol particle formation under atmospheric conditions. Proccedings of the National Academy of Science of the United States of America 107, 6646—6651.

Morawska, L., Zhang, J., 2002. Combustion sources of particles. 1. Health relevance and source signatures. Chemosphere 49, 1045—1058.

Pey, J., Querol, X., Alastuey, A., Rodríguez, S., Putaud, J.P., Van Dingenen, R., 2009. Source apportionment of urban fine and ultra-fine particle number concentration in a Western Mediterranean city. Atmospheric Environment 43, 4407—4415.

Putaud, J.-P., Raes, F., Van Dingenen, R., Brüggemann, E., Facchini, M.-C., Decesari, S., Fuzzi, S., Gehrig, R., Hüglin, C., Laj, P., Lorbeer, G., Maenhaut, W., Mialopoulos, N., Müller, K., Querol, X., Rodríguez, S., Schneider, J., Spindler, G., ten Brink, H., Tørseth, K., Wiedensohler, A., 2004. A European aerosol phenomenology—2: chemical characteristics of particulate matter at kerbside, urban, rural and background sites in Europe. Atmospheric Environment 38, 2579—2595.

Putaud, J.-P., Van Dingenen, R., Alastuey, A., Bauer, H., Birmili, W., Cyrys, J., Flentje, H., Fuzzi, S., Gehrig, R., Hansson, H.C., Harrison, R.M., Herrmann, H., Hitzenberger, R., Hüglin, C., Jones, A.M., Kasper-Giebl, A., Kiss, G., Kousa, A., Kuhlbusch, T.A.J., Löschau, G., Maenhaut, W., Molnar, A., Moreno, T., Pekkanen, J., Perrino, C., Pitz, M., Puxbaum, H., Querol, X., Rodriguez, S., Salma, I., Schwarz, J., Smolik, J., Schneider, J., Spindler, G., Ten Brink, H., Tursic, J., Viana, M., Wiedensohler, A., Raes, F., 2010. A European aerosol phenomenology-3: physical and chemical characteristics of particulate matter from 60 rural, urban, and kerbside sites across Europe. Atmospheric Environment 44, 1308—1320.

Puustinen, A., Hämeri, K., Pekkanen, J., Kulmala, M., De Hartog, J., Meliefste, K., Ten Brink, H., Kos, G., Katsouyanni, K., Karakatsani, A., Kotronarou, A., Kavouras, I., Meddings, C., Thomas, S., Harrison, R., Ayres, J.G., Van der Zee, S., Hoek, G., 2007. Spatial variation of particle number and mass over four European cities. Atmospheric Environment 41, 6622—6636.

Querol, X., Alastuey, A., Rodríguez, S., Plana, F., Ruiz, C.R., Cots, N., Massagué, G., Puig, O., 2001. PM10 and PM2.5 source apportionment in the Barcelona Metropolitan area, Catalonia, Spain. Atmospheric Environment 35, 6407—6419.

Querol, X., Alastuey, A., Rodríguez, S., Viana, M.M., Menéndez, M., Gil Ibarguichi, J.I., 2004a. Speciation and origin of PM10 and PM2.5 in Spain. Journal of Aerosol Science 35, 1151—1172.

Querol, X., Alastuey, A., Rodríguez, S., Viana, M.M., Artiñano, B., Salvador, P., Mantilla, E., García do Santos, S., Fernández Patier, R., de la Rosa, J., Sánchez de la Campa, A., Menéndez, M., Gil Ibarguichi, J.I., 2004b. Levels of particulate matter in rural, urban and industrial sites in Spain. Science of the Total Environment 334-335, 359—376.

Querol, X., Alastuey, A., Moreno, T., Viana, M.M., Castillo, S., Pey, J., Rodríguez, S., Artiñano, B., Salvador, P., Sánchez, M., García Dos Santos, S., Herce Garraleta, M.D., Fernández-Partier, R., Moreno-Grau, S., Negral, L., Minguillón, M.C., Monfort, E., Sanz, M.J., Palomo-Marín, R., Pinilla-Gil, E., Cuevas, E., de la Rosa, J., Sánchez de la Campa, A.M., 2008. Spatial and temporal variations in airborne particulate matter (PM10 and PM2.5) across Spain 1999—2005. Atmospheric Environment 42, 3964—3979.

Reche, C., Querol, X., Alastuey, A., Viana, M., Pey, J., Moreno, T., Rodríguez, S., González, Y., Fernández-Camacho, R., Sánchez de la Campa, A.M., de la Rosa, J., Dall'Osto, M., Prévôt, A.S.H., Hueglin, C., Harrison, R.M., Quincey, P., 2011. New considerations for PM, Black Carbon and particle number concentration for air quality monitoring across different European cities. Atmospheric Chemistry Physics 11, 6207—6227.

Rodríguez, S., Cuevas, E., 2007. The contributions of 'minimum primary emissions' and 'new particle formation enhancements' to the particle number concentration in urban air. Journal of Aerosol Science 38, 1207—1219.

Rodríguez, S., Van Dingenen, R., Putaud, J.P., Dell'Acqua, A., Pey, J., Querol, X., Alastuey, A., Chenery, S., Kin-Fai, H., Harrison, R.M., Tardivo, R., Scarnato, B., Gianelle, V., 2007. A study on the relationship between mass concentrations, chemistry and number size distribution of urban fine aerosols in Milan, Barcelona & London. Atmospheric Chemistry Physics 7, 2217—2232.

Rodríguez, S., González, Y., Cuevas, E., Ramos, R., Romero, M., Abreu-Afonso, J., Redondas, A., 2009. Atmospheric nanoparticle observations in the low free troposphere during upward orographic flows at Izaña Mountain Observatory. Atmospheric Chemistry and Physics 9, 6319—6335.

Rodríguez, S., Alastuey, A., Alonso-Pérez, S., Querol, X., Cuevas, E., Abreu-Afonso, J., Viana, M., Pandolfi, M., de la Rosa, J., 2011. Transport of desert dust mixed with North African industrial pollutants in the subtropical Saharan Air Layer. Atmospheric Chemistry and Physics 11, 6663—6685.

Sánchez de la Campa, A.M., de la Rosa, J., González-Castanedo, Y., Fernández-Camacho, R., Alastuey, A., Querol, X., Stein, A.F., Ramos, J.L., Rodríguez, S., García Orellana, I., Nava, S., 2011. Levels and chemical composition of PM in a city near a large Cu-smelter in Spain. Journal of Environmental Monitoring 13, 1276.

Sipilä, M., Berndt, T., Petäjä, T., Brus, D., Vanhanen, J., Stratmann, F., Patokoski, J., Mauldin, R.L., Hyvärinen, A.P., Lihavainen, H., Kulmala, M., 2010. The role of sulphuric acid in atmospheric nucleation. Science 327, 1234—1246.

Stanier, C.O., Khlystov, A.Y., nd Pandis, S.N., 2004. Ambient aerosol size distributions and number concentrations measured during the Pittsburgh Air Quality Study (PAQS). Atmospheric Environment 38, 3275—3284.

Thurston, G.D., Spengler, J.D., 1985. A quantitative assessment of source contribution to inhalable particulate matter pollution in Metropolitan Boston. Atmospheric Environment 19, 9—25.

Turpin, B.J., Lim, H.J., 2001. Species contribution to PM2.5 mass concentrations: revisiting common assumptions for estimating organic mass. Aerosol Science and Technology 35, 602—610.

WHO, 2005. Air Quality Guidelines Global Update. http://www.euro.who.int/Document/E90038.pdf.